

AUTOMATIC FLC-VALUE DETERMINATION FROM 4D STRAIN DATA

P. Feldmann¹, M. Schatz¹, and P. Aswendt¹

¹ ViALUX Messtechnik + Bildverarbeitung GmbH
Am Erlenwald 10, D-09128 Chemnitz, Germany
e-mail: autogrid@vialux.de, Web page: www.vialux.de

ABSTRACT

Advanced optical strain analysis technologies permit in-process image recordings during the FLC tests. This functionality offers the advantage to record image sequences directly including also the beginning of the material failure – beginning of local necking followed by the crack. In general experimental strain analysis is able to provide exact results only for continuous deformation fields (before local necking or cracks).

One important topic is the reliable determination of FLC values by evaluation of Nakajima and Marciniak tests. These tests and their evaluation have been standardized in the latest ISO 12004 version [1]. This presentation describes the evaluation of 4D (time depending) strain data. The presented automatic algorithm is a reliable and operator independent method to determine FLC values from the recorded and analyzed time sequence images. Its application is demonstrated for various typical up to date sheet metal materials. Additionally, the results are compared with the position dependent method using intersections described in ISO 12004 [1] part 2 and with an alternative time dependent evaluation method based on strain rate frequency diagrams developed by Volk et al. [2].

Keywords: Sheet metal forming, optical 4D strain analysis, evaluation of FLC tests

1. INTRODUCTION

Forming limit curves represents major strains as a function of minor strains under the assumption of a straight strain path when the material failure (local necking followed by a crack) starts. The most sophisticated task in FLC testing is the exact determination of strains at the beginning of the local necking followed by the crack. ISO 12004 [1] part 2 describes a position dependent method using intersections to determine FLC value pairs for the beginning of the material failure. However, it is working with no real access to that moment before the material failure starts to determine the forming limits directly at this moment. Besides the results become completely unstable in the case of more than one local maximum that can typically occur during FLC testing.



Figure 1. Strain analysis system AutoGrid[®] integrated into ERICHSEN testing machine for FLC tests

The integration of advanced strain analysis systems into testing machines (see Figure 1) and their capability of in-process recording of image sequences during the FLC tests opens the chance to get direct access to the forming history before and during local necking till the crack appears. Such experimental setup enables to determine reliable FLC values automatically. The rules described in ISO 12004 are referring to the time depending evaluation of FLC tests: “The evaluation of the time dependent method is at present carried out and could be added during the next revision of the document.” Actually, the major challenge is the reliable and operator independent identification of the beginning of local necking in the recorded and analyzed image sequences for a wide range of sheet metal materials. This paper presents an automatic algorithm for the determination of FLC values from image sequences.

The analysis only takes a few minutes for the whole image sequence. Figure 2 shows the results of the image set before the local necking starts. Additionally, the strain paths of two neighbouring points are shown in black color. It becomes obvious, that only the growth of the major strain value φ_1 till the end of the image sequence does not sufficiently indicate the beginning of the local necking.

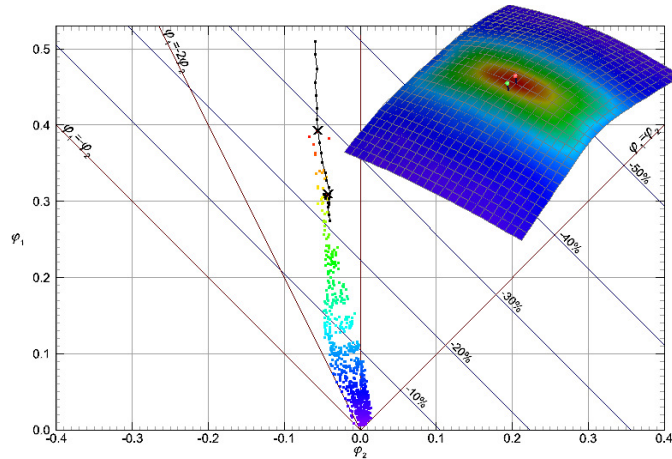


Figure 2. Strain results before start of the local necking including the strain paths of two marked points

Looking at the strain path of the second marked point - the direct neighbour of the “maximum point”- shows the following effect: This strain path reaches its maximum not at the end of the analyzed sequence. The strains are approximately constant over the last steps. This signal indicates clearly that at the beginning of the analyzed image sequence the major strain value increases and then the deformation stops. Reason for that is that any material elongation in the direct neighbourhood of the necking area towards the necking zone is impossible when local necking starts. Figure 3 shows the incremental strains during local necking. A necking zone (green marking) consists of a thin local necking area itself (red) and accompanying stopping areas (light blue) on both sides. The evaluated strain fields give a precise picture of this phenomenon.

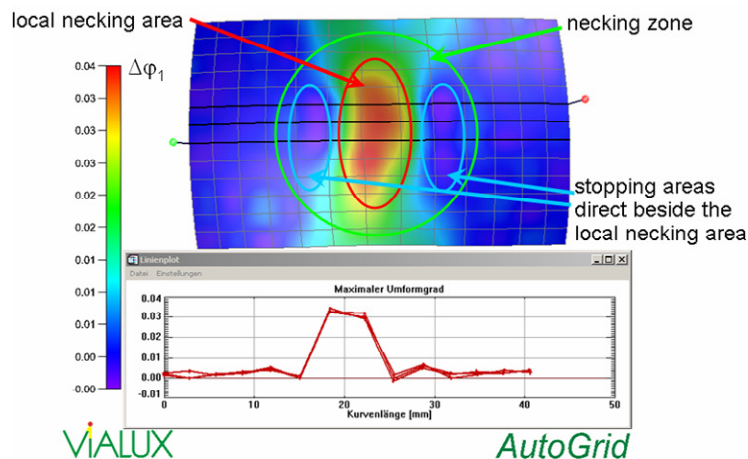


Figure 3. Incremental major strain $\Delta\varphi_1$ distribution over the whole area and along intersections during necking: stopping areas on both sides of the necking zone

2. ALGORITHM FOR AUTOMATIC DETERMINATION OF FLC-VALUES FROM IMAGE SEQUENCES

After FLC test an image sequence is recorded including images before and during local necking till the crack appears. The following chapter gives a detailed description of the developed approach for the automatic identification of the last image set before the beginning of local necking. A first presentation of this methodology was given at the Zurich FLC conference in 2006 [3].

The approach should meet the following requirements:

- fully operator independent,
- automatic operation,
- high reliability based on internal reliability checks,
- applicable to a wide range of materials and
- ease of use.

Actually, this algorithm is available as an Excel Macro. It can be applied by all users of strain analysis systems using their own data basis. The approach is also integrated into the AutoGrid[®] evaluation software for FLC testing [4].

The developed algorithm includes the following steps:

Step 1: Selection of the last image set before the crack gets visible in the image sequence

These images normally show a clear local necking but still no signs of a crack. This position has to be marked over maximal five coherent grid stitches.

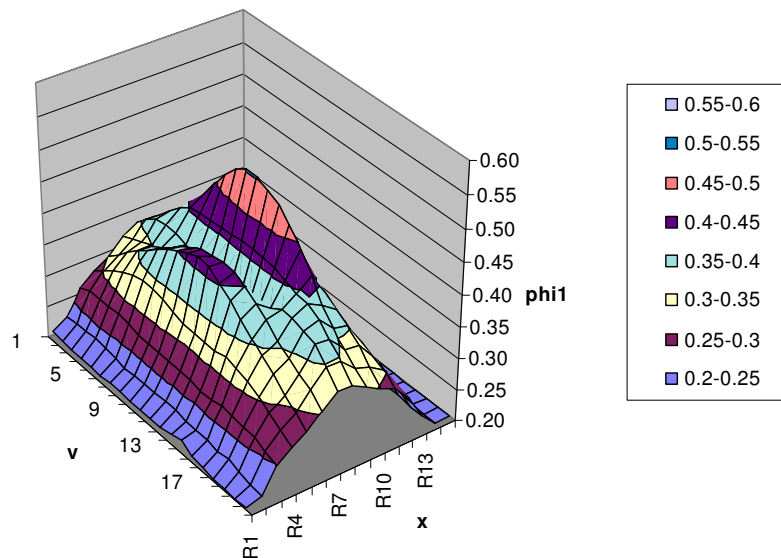


Figure 4. Strain distribution in the last image set before the crack; identification of the local necking area

Step 2: Evaluation of at least 20 image sets before the first image set with a visible crack, including image sets before and during local necking

The strain values of all analyzed image sets along the same intersection perpendicular to the local necking area are shown in Figure 5. There is a difference in the step width between the local necking area (grid point $u=9$), the stopping areas on both sides (left: $u=7$; right: $u=11$), and the flawless area of the specimen.

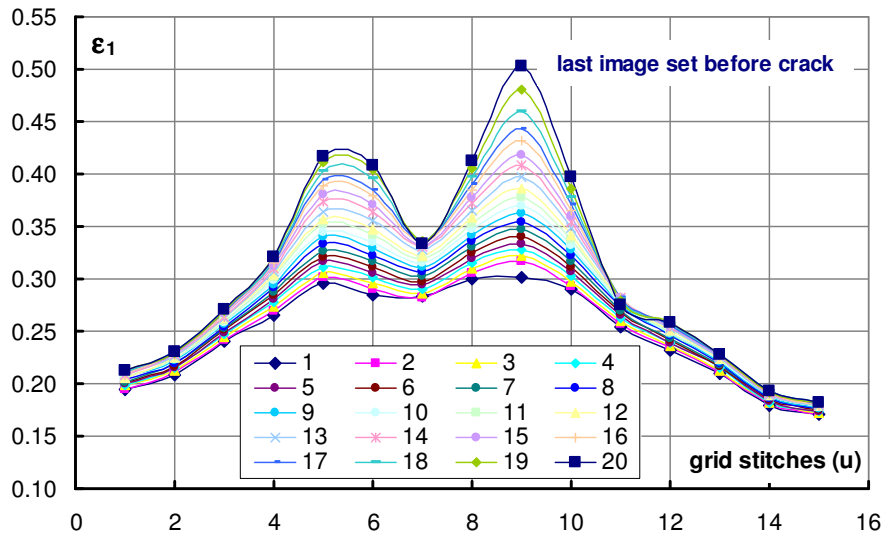


Figure 5. Major strains along intersections perpendicular to the local necking area results before start of the local necking

Step 3: Calculation of mean values of major strain for all point triples on both sides of the determined maximum point triple

Figure 6 shows the calculated mean values depending upon the sequence index. During a time sequence the major strain ϕ_1 increases significantly in the area where the crack will occur ("maximum"). Local necking is characterized by a higher rate of strain growth compared to the surrounding area. Fields with stopping deformation occur on both sides of the maximum. The example in Figure 5 and 6 shows this behavior at "u=7" on the left and "u=11" on the right side.

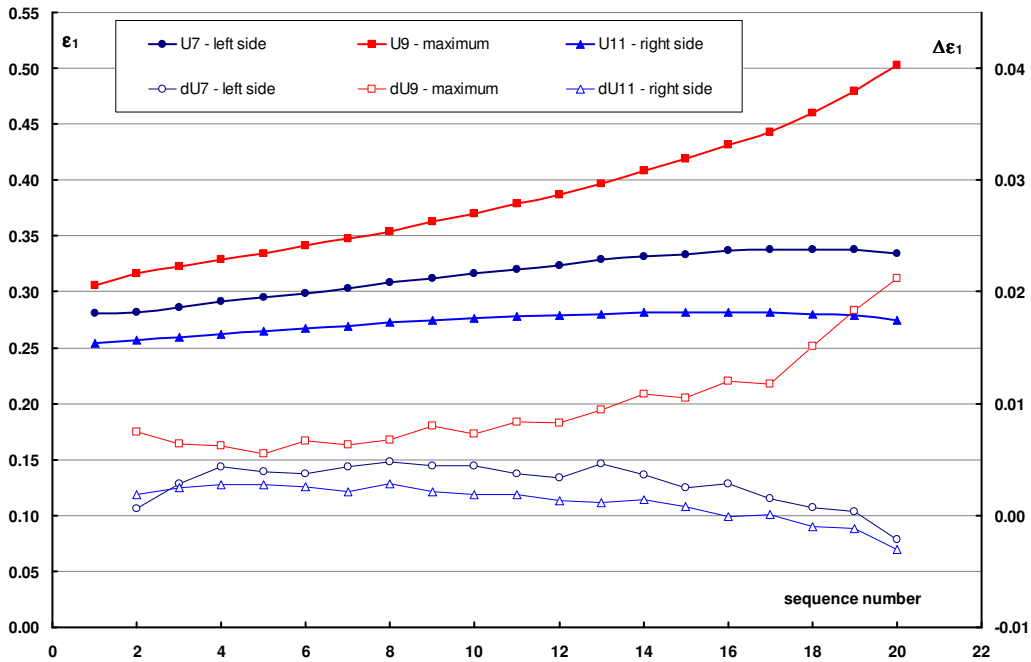


Figure 6. Time courses of mean values and increments

Step 4: Calculation of the difference of the deformation increments (similar to strain rates) between the maximum and the stopping environment for both sides
 After a continuous growth till sequence number 10 the strain difference increases considerably (Figure 7).

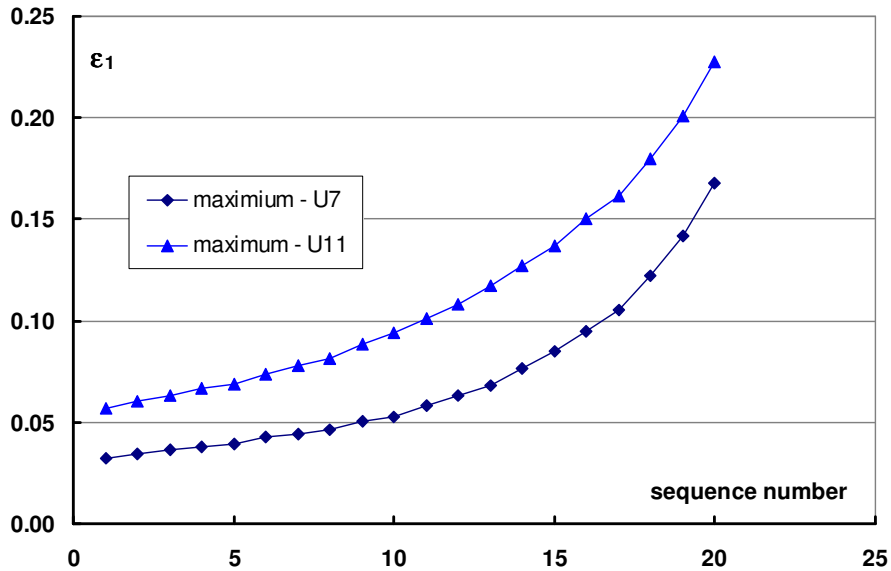


Figure 7. Time course of the differences of major strain increments (maximum – left side U7; maximum – right side U11)

Step 5: Assumption: The rise of these differences is linear in the period before the beginning of local necking.
 The strain increases progressively at the beginning of local necking. Therefore the linear differences of the major strain φ_1 are calculated step-by-step. Figure 8 shows the fitting line for the first seven values.

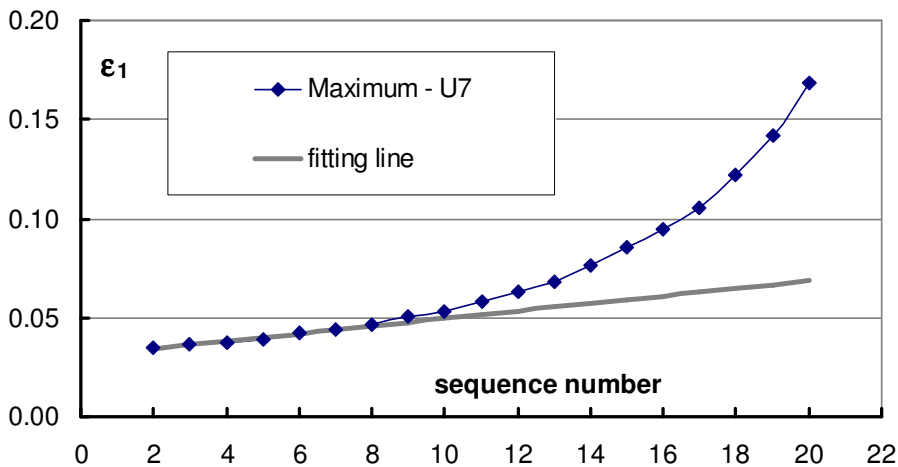


Figure 8. Fitting line from the 2nd to the 8th value

The correlation coefficients of both sides are shown in Figure 9. The peak values are marked. The linear field is determined up to the best correlation. The number of points for the calculation of the fitting line for the linear section is determined for both sides. To guarantee a high degree of reliability the correlation coefficient has to be >0.9 , otherwise the automatic algorithm stops and gives a message on the display.

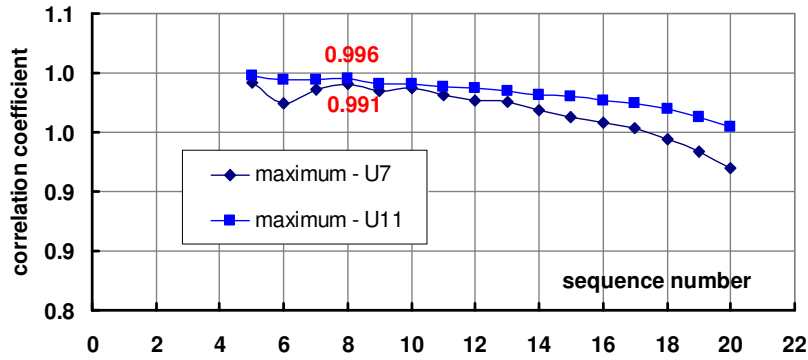


Figure 9. Correlation coefficient of both sides depending upon the number of considered values

Step 6: Next, the standard deviation of the incremental major strain values is calculated for the determined linear section to consider the spread caused by the material, the experimental conditions and the measuring inaccuracy.

Step 7: To determine the last image set before the beginning of material failure unambiguously, an upper boundary line is defined parallel to the linear fitting line. It is shifted upwards by factor 3 of the standard deviation determined in step 6. The first image set above this upper boundary is defined as the image set with starting of local necking. Thus, one image set before is the image set for the evaluated side. In Figure 10 image set 11 indicates the first one above the upper boundary line. Detected by the difference values of the left side the 10th image set is the one before local necking starts.

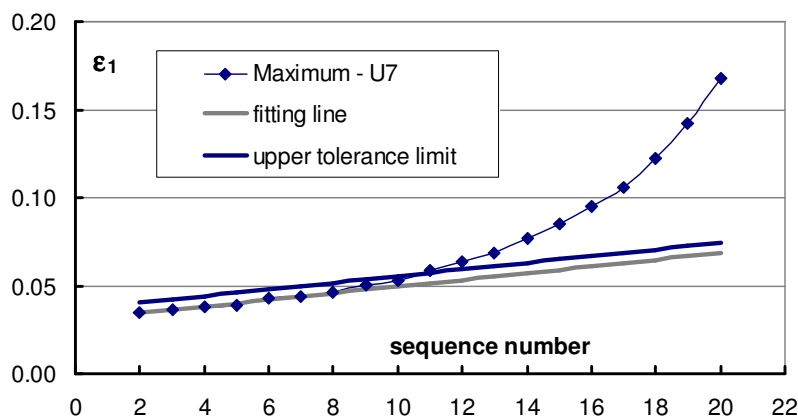


Figure 10. Upper tolerance line parallel to the fitting line of the linear period

This step has to be repeated for the other side (in the example: maximum – value (U=11)). That means, the algorithm includes an independent reliability check: If the same image set is

determined for both sides, the degree of reliability is high. Otherwise, if the determined image sets differ by one image set, the degree of reliability is still sufficient. In this case the determination of the FLC values takes place on that side, where the linear fitting line could be described with the higher correlation coefficient. If the difference between left and right side is more than one image set, the automatic algorithm stops. The operator is informed that the last image set before the start of local necking has to be determined manually.

Step 8: Calculation of FLC-value-pairs

The image set before the material failure starts has to be determined. In the marked area of the crack (step 1) the mean value of the maximum of 3 (2.0-mm grid) or 2*6 (1.0-mm grid) coherent points is the major strain value for the FLC. The mean value of the minor strains has to be calculated also based on these points to complete the FLC-value-pair.

3. COMPARISON OF SELECTED EXAMPLES EVALUATED BY THE THREE DIFFERENT METHODS

3.1 Preliminary Remarks

The German IDDRG working group for standardization of FLC determination [1] has carried out a great quantity of round robin tests using identical steel and aluminum sheet metals in different material testing laboratories. The following examples were included in these round robin tests. Three different methods – the position dependent method using intersection lines [1] and both time dependent methods [2, 3] – were applied on identical image sets from the same experiment to ensure the same data base for comparison.

Three different materials were investigated:

- DC05+ZE (1.0312 a low carbon non alloy steel),
- FB-W[®] 600 (1.8949 hot strip high-strength multiphase steel) and
- TRIP 700 high-strength steel.

All testing parameters followed the ISO 12004 [1] descriptions. A hemispherical 100 mm diameter punch was used. Each specimen was marked with 2.0 mm square line grid. In the following figures the position dependent method using intersection lines [1] is called “method 1”. The described time dependent method based on the strain differences between the local necking and the stopping areas [3] is named “method 2”, and the time dependent method based on strain rates frequency diagrams [2] is called “method 3”.

3.2 Comparison for DC05+ZE

At first the evaluation methods were applied on a typical sheet metal material with high formability. It shows homogenous deformation until the characteristic local necking starts. There occurs only one maximum that gives a good basis for the comparison of the three methods. Figure 11 shows the FLC-results of the evaluated five shapes of specimen. The mean values of three specimens from each shape and the single standard deviations (rms) of the values are displayed in the FLD.

Specimen shapes “b”, “c”, and “d” show no significant variation, the results of all three methods are very close to each other. The standard deviation of three specimens per shape is low. The three different evaluation methods proved well suited. The shape “a” specimen does not correspond to the expected forming behavior that higher major strain values are obtained for shape “a” compared to “b”. Here, only method 2 leads to reasonable results. Both time dependent methods yield reliable results in the biaxial case shape “e”. Method 1 gives a difference ($\varphi=0.5$) whereby the values do more spread.

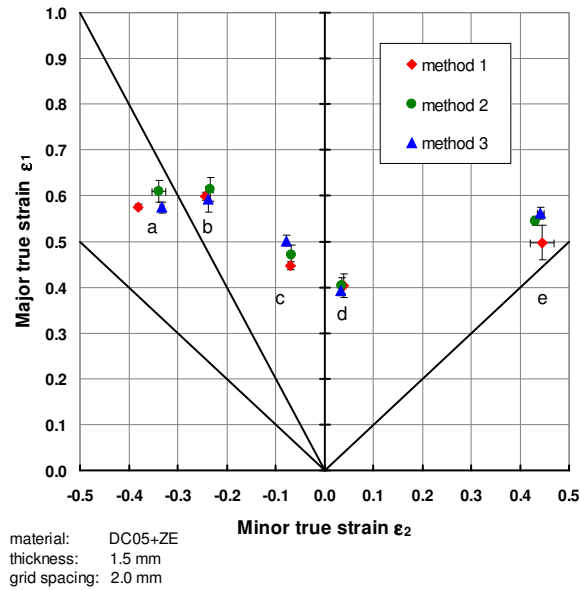


Figure 11. Comparison of FLC values for DC05+ZE determined by the three methods

The application of all three methods for specimen shape “c” is illustrated in the next figures. Figure 12 shows the evaluation with method 1 using three intersection lines. One maximum is located in the centre, and a homogenous strain distribution along the intersections becomes obvious. The major strain fitting functions for all three intersection lines are nearly identical and follow the real major strain courses in the fitting windows on both sides. There is a clearly defined signal of the maximum of the 2nd derivatives. This perfectly meets the basic ideas of the position dependent approach and the results correspond to both time dependent methods.

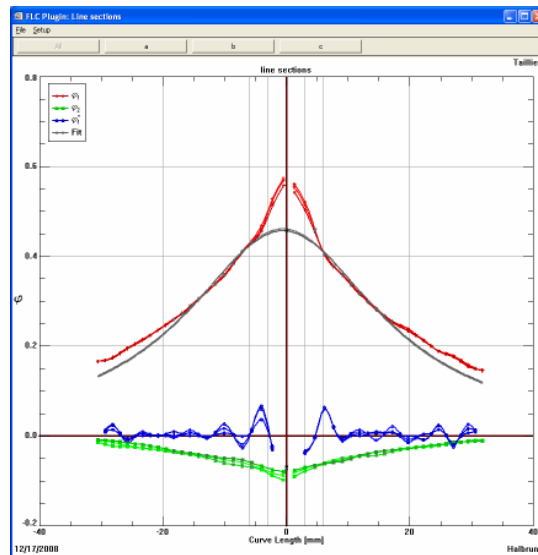


Figure 12. Determination of FLC values – method 1

In Figure 13 the results of FLC value determination are illustrated for method 2. The diagrams show the development on both sides of the maximum depending upon sequence number. Image set 9 is identified as image set before the start of local necking for the left side

(upper diagram). Image set 10 is determined for the right side. The reliability condition of the algorithm is fulfilled because of only one image set difference. The courses of strain differences are smooth before and during local necking. Due to the better correlation coefficient image set 9 is used for FLC value determination.

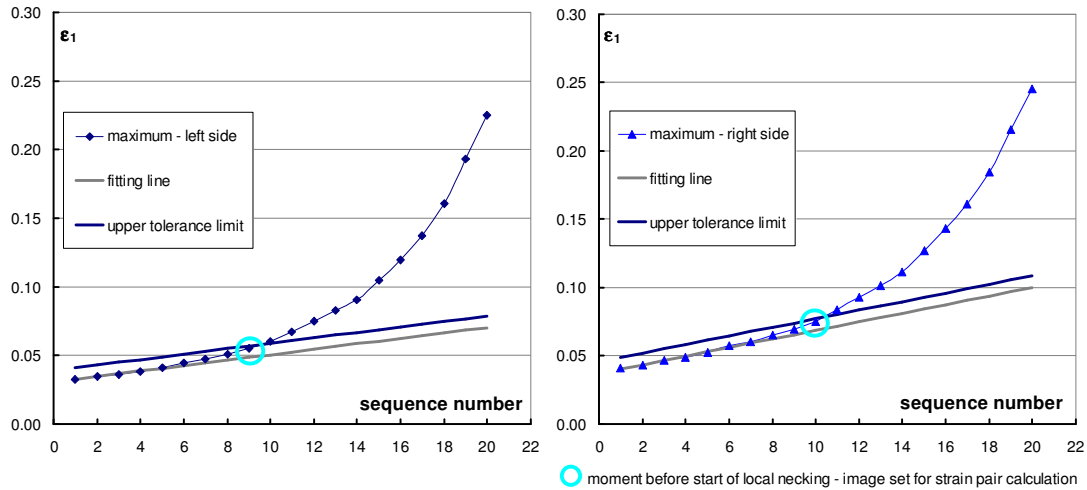


Figure 13. Determination of FLC values – method 2

Results of method 3 are demonstrated in Figure 14 [2]. Again, this algorithm can be executed as Excel macro with open user interface. The calculated strain rates for 40 deformation steps (diagram lines) are sorted by size-classes (columns). If the number of grid elements with higher strain rate values increases significantly the automatic algorithm determines the last image set before the start of local necking. Then the average of the five highest major strain values is calculated as FLC value. The FLC value pair is completed by minor strain as average of the minor strain values of the same points. The comparison shows that method 3 results in FLC values only with small deviation to the results obtained by the other methods.

	0 - 0,0263	0,0263 - 0,0526	0,0526 - 0,0789	0,0789 - 0,1052	0,1052 - 0,1315	0,1315 - 0,1577	0,1577 - 0,184	0,184 - 0,2103	0,2103 - 0,2366	0,2366 - 0,2629	0,2629 - 0,2892	0,2892 - 0,3155	0,3155 - 0,3418	0,3418 - 0,3681	0,3681 - 0,3944	Delta ε ₁ 5	ε ₁ average max 5	ε ₂ average max 5
0,1	69	53	4													0,0037	0,2702	-0,0344
0,2	69	53	4													0,0051	0,27392	-0,0343
0,3	72	54														0,0038	0,27903	-0,0355
0,4	71	55														0,0046	0,28285	-0,0369
0,5	72	54														0,0055	0,2875	-0,0384
0,6	72	54														0,0045	0,29301	-0,0395
0,7	69	57														0,0034	0,29754	-0,04
0,8	66	60														0,0049	0,30097	-0,043
0,9	60	66														0,0057	0,3059	-0,0439
1	66	60														0,0054	0,31164	-0,0447
1,1	64	62														0,0054	0,31702	-0,0451
1,2	63	63														0,0057	0,3224	-0,0474
1,3	58	67	1													0,0059	0,32814	-0,0487
1,4	60	65	1													0,0059	0,33399	-0,0497
1,5	60	66														0,0060	0,33986	-0,0508
1,6	62	64														0,0067	0,34581	-0,0525
1,7	59	65	2													0,0059	0,35248	-0,0541
1,8	61	58	7													0,0068	0,3584	-0,0549
1,9	63	56	7													0,0076	0,36518	-0,0567
2	64	47	15													0,0074	0,37279	-0,0582
2,1	64	41	21													0,0068	0,38023	-0,0593
2,2	63	41	22													0,0084	0,38702	-0,0603
2,3	67	37	22													0,0086	0,39543	-0,0627
2,4	68	32	26													0,0077	0,40399	-0,0644
2,5	65	34	28	1												0,0092	0,41165	-0,0666
2,6	67	30	28	1												0,0102	0,42089	-0,0678
2,7	71	27	20	8												0,0103	0,43108	-0,0691
2,8	70	23	19	14												0,0104	0,44142	-0,0708
2,9	72	22	17	15												0,0134	0,45163	-0,0755
3	75	21	14	12	6											0,0120	0,46524	-0,0757
3,1	75	20	13	7	11											0,0130	0,47726	-0,0768
3,2	76	21	11	4	10	4										0,0169	0,49021	-0,0787
3,3	84	14	10	1	9	8										0,0175	0,50708	-0,0814
3,4	88	15	5		3	9	4	3								0,0186	0,52458	-0,0829
3,5	89	17	2		3	4	4	3	4							0,0224	0,54314	-0,0867
3,6	96	12			1	7	2	3	4							0,0330	0,56556	-0,0886
3,7	103	5	1		1	1	1	1	4	7						0,0330	0,5986	-0,0912
3,8	106	2	1		1	1	1	1	1	6	3	2	2			0,0258	0,63159	-0,0933
3,9	103	5	1		1	1	1	1	1	1	2	2	9			0,0502	0,65739	-0,0927
4	74	29	4	2	1	1	1	1	2				1	1	11	0,7076	-0,0958	

Figure 14. Determination of FLC values with strain rates in a frequency diagram (method 3)

3.3 Comparison for FB-W 600

The results for this well formable steel show for each of the 10 different specimen shapes a significant lower FLC- ϕ_1 -value of the position dependent method 1 compared to both time dependent methods. This deviation is caused by the impossible access to the moment of the start of local necking. The intersection line method indicates more conservative FLC values. The time dependent methods 2 and 3 show that such smaller FLC values do not correspond to the real material behavior. There is a continuous forming process without unstable local necking.

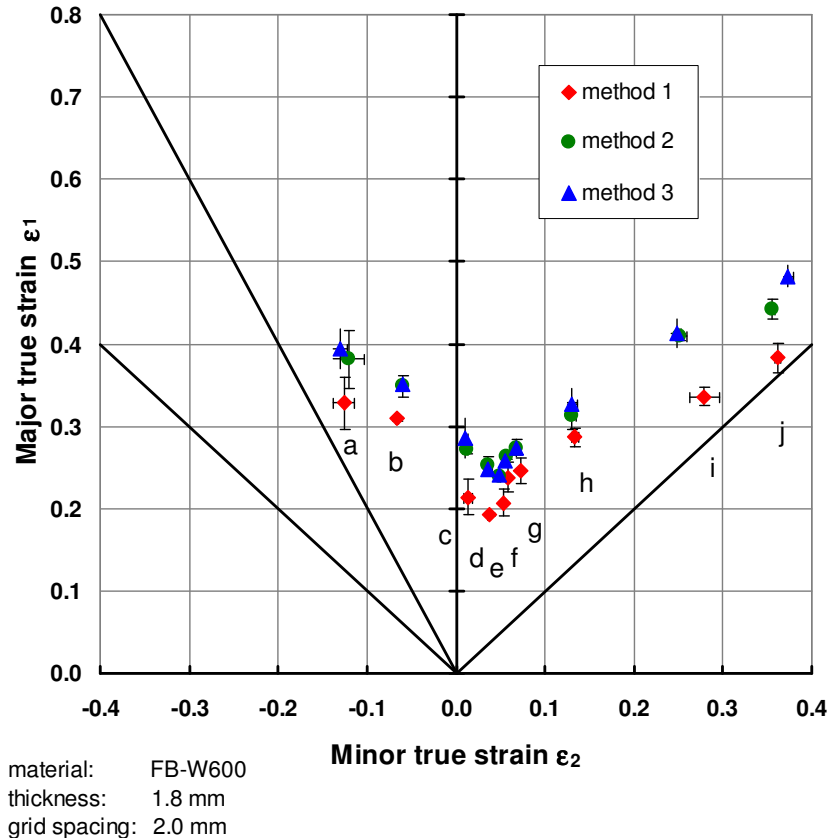


Figure 15. Comparison of FLC values for FB-W 600

All 10 shapes of specimen show no significant variation between both time dependent methods. Again, the two methods provide nearly the same results computed on complete different ways. This is an additional sign for the reliability of these results determined by time dependent methods. The next figures illustrate special differences between FB-W 600 and DC05+ZE. The application of the 3 methods is demonstrated on specimen shape “b”.

The intersection lines used by method 1 yield a more inhomogeneous strain distribution with stronger localization. The fitting function is not able to follow the real major strain courses especially on the inner side of the fitting windows. Thus, the fitting algorithm fails in finding the corresponding higher values of major strain.

Furthermore, the maximum of the 2nd derivatives is not at the same position in all three sections on the right side. This leads to different inner borders of the fitting window on this side. In this case the fitting functions of all three intersection lines (displayed in grey color) do not match in course and maximum.

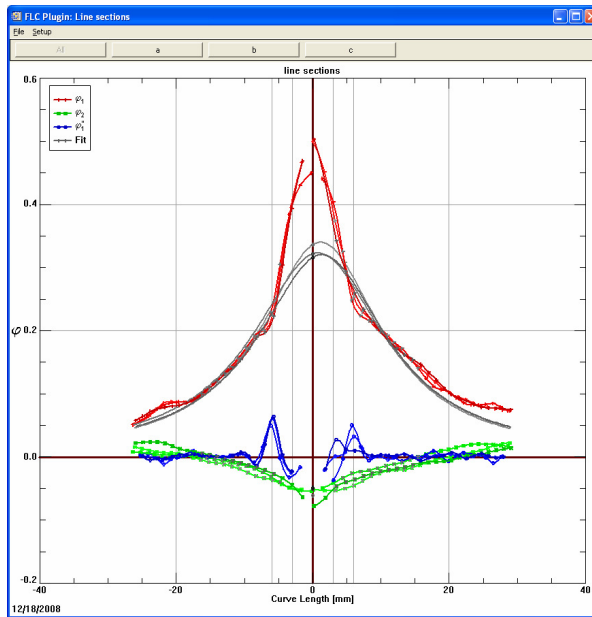


Figure 16. Determination of FLC values – method 1

The results for method 2 are shown in Figure 17. Here, the upper boundary blue line helps to separate normal data scatter from the real beginning of local necking. Another difference is the higher gradient of the fitting line compared to DC05+ZE caused by the faster localization of higher strains in the center. But these facts have no influence on the stability of the algorithm. Image set 10 could be selected at both sides confirming the reliability check. The same picture set is also determined by the frequency diagram based method 3.

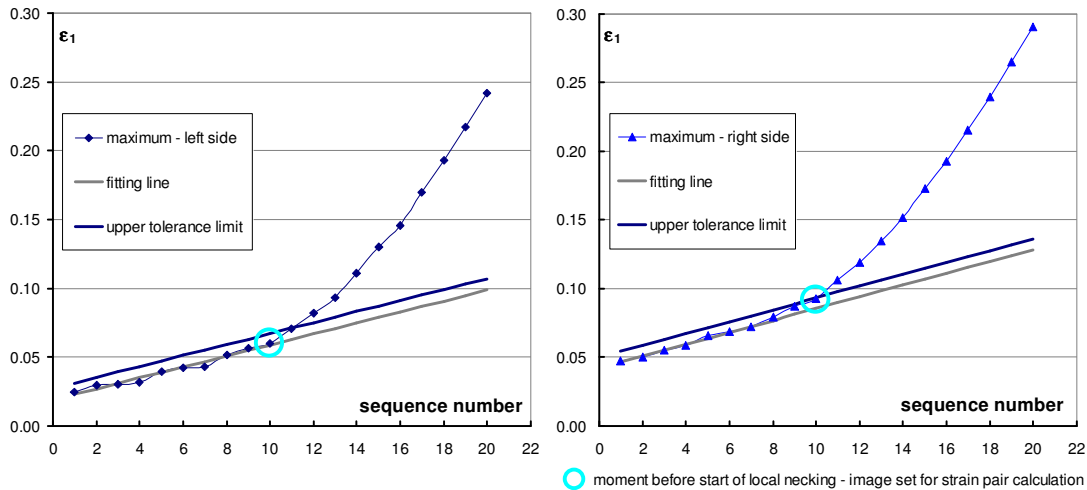


Figure 17. Determination of FLC values - method 2

3.4 Comparison for TRIP 700

TRIP 700 (thickness 1 mm, approx. plain strain) was selected to show the influence of the occurrence of more than one maximum in the necking zone. The typical strain distribution is visible in Figure 18. The fitting function of method 1 is not able to approximate the real course

of the major strains. The major strain FLC results become unreliable depending on the accident course of major strain in the neighborhood of the central maximum. Usually, such application cases should be excluded for method 1 by the operator.

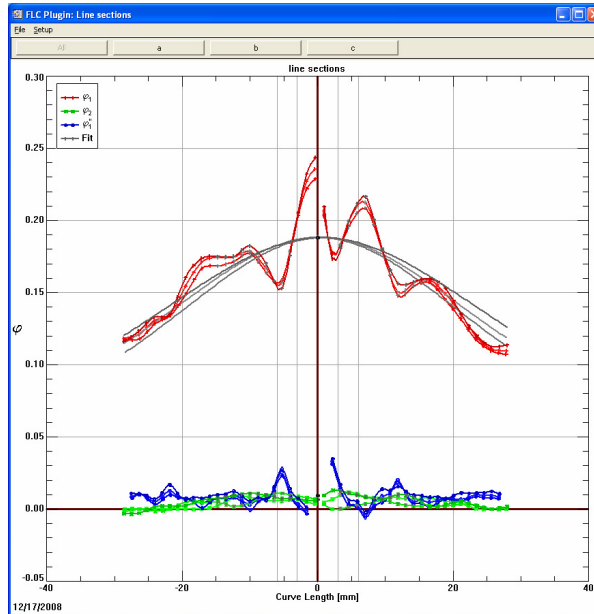


Figure 18. Determination of FLC values – method 1

Figure 19 displays the FLC value determination applying method 2. Now, additional maxima cause no problem for the evaluation, because only the strain values in the identified local necking zone (the maximum and the both stopping areas in the direct neighborhood) are used. The algorithm selects image set 15 on the left and set 14 on the right side. The difference of one image set fulfils the reliability test. Due to the higher correlation coefficient on the right side the strain values from image set 14 (equal to the 7th last image set before cracking) are used for FLC value determination. In this way an FLC- ϕ_1 -value of 0.22 is determined. The 2nd maximum on the right side (Figure 18) demonstrates that unstable local necking does not start if $\phi_1 \leq 0.22$.

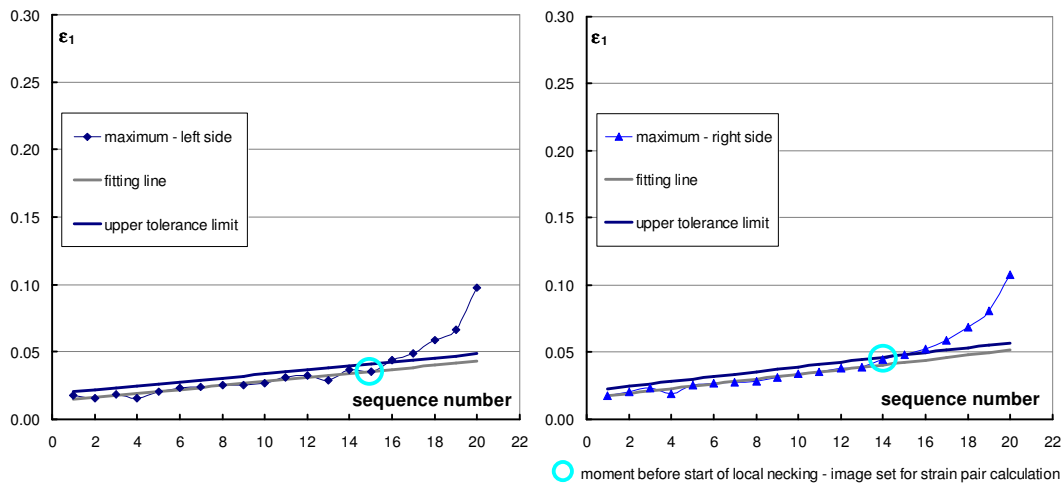


Figure 19. Determination of FLC values - method 2

The same result is given by method 3. The algorithm determines the 7th last image set before cracking for FLC value determination. But it becomes obvious that method 3 is not capable to identify the position of the crack. Especially in the case of more than one maximum in the affected material region it can occur that invalid points - not related to the cracking zone - are selected for FLC value calculation. So, the operator should check the results of method 3.

4. CONCLUSIONS AND OUTLOOK

The paper presented a comparison of three methods to obtain reliable strain data in FLC testing. Alternatively to the time dependent evaluation method of Volk et al. [2] the algorithm of a second time dependent evaluation method was described in detail. It is based on the recording and automatic evaluation of time sequences and gives the possibility to analyze the phenomena of unstable local necking by a precise identification of really influenced grid markings in the critical crack region. The application of this method was demonstrated on typical materials and compared with the position dependent evaluation method described in ISO 12004 [1] and the second time dependent evaluation method.

The results have shown that the new method provides reliable FLC data also considering “strong localization of the necking zone” and “more than one maximum”. In these cases the position dependent method fails and the second time dependent method needs the operator to audit the frequency diagram to be confident of the affected region. However, both time dependent methods offer the potential for an automatic reliability check.

The performance as well as the convenient use of the new time dependent methods will help to address an increasing number of experts in this field. Especially the implementation of these algorithms in commercially available strain analysis systems makes it easier to operate.

Future investigations will focus on the following issues:

- high temperatures and
- instable forming behavior of materials

to overcome existing limitations.

5. ACKNOWLEDGEMENTS

We like to thank Dr. W. Volk, R. Illig and H. Kupfer from BMW and Dr. L. Kessler, Dr. J. Gerlach and A. Koehler from ThyssenKrupp for their kind support with experimental data.

6. REFERENCES

1. Metallic materials – Sheet and strip – Determination of forming limit curves – Part 2: Determination of forming limit curves in laboratory (ISO 12004-2). ISO copyright office, Geneva 2006.
2. B. Eberle, W. Volk, P.Hora: “Automatic approach in the evaluation of the experimental FLC with a full 2d approach based on a time depending method”, Proceedings of Numisheet 2008, Interlaken, 279 – 284.
3. P. Feldmann, M. Schatz: “Effective evaluation of FLC tests with the optical in-process strain analysis system AutoGrid[®]”, Proceedings of the FLC Zurich 2006, 15th – 16th March 2006, IVP, ETH Zurich, Switzerland.
4. “Strain Analysis System AutoGrid[®] – Operator’s manual”, ViALUX Messtechnik & Bildverarbeitung GmbH, Chemnitz, 2008.